Third-Order Nonlinear Optical Properties of Sulfur-Rich Compounds

Jonathan G. Breitzer,* Dana D. Dlott, Lawrence K. Iwaki, Sean M. Kirkpatrick,† and Thomas B. Rauchfuss

School of Chemical Sciences, Chemical and Life Sciences Laboratory, University of Illinois at Urbana−Champaign, Urbana, Illinois 61801

Received: January 11, 1999; In Final Form: April 19, 1999

The molecular third-order optical nonlinearity γ_R (second hyperpolarizability or nonlinear refractive index) was measured for a series of sulfur-rich molecules: sulfur (S_8), carbon−sulfur compounds, and metal thiolate clusters. *Z*-scan techniques (pulse width 27 ps, wavelength 527 nm) were used to measure these properties in solution by comparing the solution to the pure solvent. Our approach is an efficient way to evaluate a number of different compounds and to quickly direct synthetic strategies for improved nonlinear and linear optical properties. The optical nonlinearities were evaluated in terms of figures of merit, $|W|/I_0$ and $[T]^{-1}$, where $|W|/I_0$ is the ratio of nonlinear refraction to linear absorption and $[T]^{-1}$ is the ratio of nonlinear refraction to nonlinear absorption. Among the carbon−sulfur compounds, $C_6S_8O_2$ had the largest figures of merit: $|W|/I_0 = 4.3 \times 10^{-13}$ m^2 W^{-1} and $[T]^{-1} > 5$. The metal thiolate cluster with the largest second hyperpolarizability was $[Zn_{10}S_4(SPh)_{16}]^{4-}$ ($\gamma_R = -7.8 \times 10^{-56}$ C m^4 V^{-3}, -6.3×10^{-31} esu). This cluster exhibited no measurable linear or nonlinear absorption, so the figures of merit were effectively infinite. Previous work on the second hyperpolarizability of sulfur-rich compounds examined species that were hampered by substantial linear absorption coefficients. The present work shows that high figures of merit can be achieved without significant linear or nonlinear absorption.

Introduction

The prospect of applying the molecular level control inherent in organic and organometallic syntheses has motivated many chemists to pursue the development of new second- and third-order nonlinear optical (NLO) materials. Indeed, many molecular organic and organometallic compounds have been shown to possess large molecular hyperpolarizabilities. Furthermore, it has been shown that macroscopic assemblies of these species exhibit sizable second-order ($\chi^{(2)}$) or third-order ($\chi^{(3)}$) optical nonlinearities.[1]

An ultimate practical goal for designing molecules with large third-order nonlinearities is to incorporate them into devices used in all-optical signal processing.[2] Realization of this goal entails recognizing that the molecule must not only have a large, fast optical nonlinearity ($\chi_R^{(3)} > 10^{-30}$ C m V^{-3}, 10^{-11} esu), these species must also have a small absorption, be it linear or nonlinear. A low absorbance is necessary; otherwise, slower photothermal effects dominate the desirable fast photorefractive effects and the optical damage threshold may be unacceptably low. Although not considered here, additional practical considerations influence the selection of materials for NLO applications, including factors related to processability and chemical stability.

Figures of merit[3] have been used to evaluate how well a molecule satisfies the requirement of a large nonlinear refractive index and small absorption. One does not wish to synthesize a molecule and then fabricate the NLO material, for example, by polymerizing or crystallizing it, only to find that the material's absorptive properties outweigh its useful refractive properties. In this work, we evaluate the NLO properties of candidate molecules as solutions, correcting for the contributions of the solvent. With this method, we can choose any convenient solvent for a particular sample, so it allows us to survey the optical properties of a wide range of molecules.

Ideally, NLO measurements would probe the nonlinear refraction and absorption of the candidate molecules at all pulse widths and at all wavelengths. While this is usually not practical because of instrumental limitations, we stress the importance of making the NLO measurements with ultrashort light pulses (picoseconds or less) in order to obtain the intrinsic contribution to $\chi^{(3)}$ and to choose a wavelength region that holds practical interest. In the present case, we chose to work at 527 nm in order to evaluate materials for visible wavelengths in which there exists interest for switchable holographic filters and refractive optical limiters.[4] In addition, tabulated data at a nearby wavelength of 532 nm, at about the same pulse duration, exist for some of the solvents used here, enabling us to verify our measurement technique. The use of 27 ps pulses allows us to measure contributions to $\chi^{(3)}$ arising from electronic response and molecular reorientation. Other effects such as electrostriction and thermal lensing are much slower, and we wish to avoid measuring their effects because they are not relevant to the properties of useful fast-response devices. The build-up times for these effects are roughly equal to d/c, the laser-beam diameter divided by the acoustic velocity.[5] For the 40 μm diameter beam used here and a typical acoustic velocity of 4 km/s, the build-up times are about 10 ns, which are too slow to affect our measurements. However, the decay of a thermal lens via thermal diffusion can be much slower than the build-up; in fact, it may be as slow as several milliseconds. If the laser repetition rate is too large, undesirable cumulative effects emerge. Two methods can be used to eliminate these cumulative effects of

* Author to whom correspondence should be addresssed.
† Present address: Air Force Research Laboratory, AFRL/MLPJ Bldg. 651, 3005 P ST STE 1, WPAFB, OH 45433-7702.

10.1021/jp990137f CCC: $18.00
Published on Web 08/13/1999

thermal lensing. Either the time between pulses can be made much longer than the thermal lens decay time or a flowing sample can be used. In our work, we chose to use a high repetition rate (640 Hz) to maximize our signal-to-noise ratio, so we cycled the liquid sample through a flow cell fast enough (about 150 mL/min, 25 cm/s linear velocity) to ensure a fresh sample volume for each pulse.

The present work was premised on two ideas: that sulfur anions and organosulfur compounds are known to be quite polarizable—large, conjugated sulfur-containing molecules (e.g., the tetrathiafulvalenes[6]) especially so—and that highly polarizable species tend to exhibit large second hyperpolarizabilities. The latter idea is supported qualitatively by previous third-order NLO studies on polydiacetylene,[7] oligothiophenes,[8] and carotenoids.[9] This paradigm has led to recent studies on organotransition metal complexes.[10] We were interested in extending these studies to "sulfur-rich" molecules, i.e., molecules where there is a high atomic concentration of S.[11] Carbon disulfide can be regarded as a prototypical sulfur-rich molecule, and it has long been used as a standard in third-order NLO studies. This work provides specific examples and general insights into how sulfur-rich molecules may be tailored for NLO applications while purposefully minimizing the nonlinear absorption to achieve a favorable figure of merit.

Theoretical Section. We assume our measurements are dominated by the bulk third-order susceptibility $\chi^{(3)}$. Of course, $\chi^{(2)}$ and $\chi^{(4)}$ vanish in liquids, and higher-order odd terms such as $\chi^{(5)}$ should be negligible compared to $\chi^{(3)}$. The real part, $\chi_R^{(3)}$, gives rise to an intensity-dependent phase change, i.e., a nonlinear refraction. The imaginary part, $\chi_I^{(3)}$, gives rise to an intensity-dependent amplitude change, i.e., a nonlinear absorption. These susceptibilities are given (in SI units) in terms of the nonlinear refractive index, n_2^I, and the nonlinear absorption coefficient α_2,

$$\chi_R^{(3)} = 2n_2^I n_0^2 \epsilon_0^2 c \tag{1}$$

and

$$\chi_I^{(3)} = \frac{10^8 n_0{}^2 \alpha_2 \epsilon_0}{2\pi k c} \tag{2}$$

where n_0 is the ordinary refractive index, c the velocity of light, and k the magnitude of the wave vector, $k = 2\pi/\lambda$, where λ is the wavelength.[12]

In our experiments, we measure the nonlinear refraction n_2^I and the nonlinear absorption coefficient α_2 for a dilute solution containing a known mole fraction f of solute. We also measure the same properties for the pure solvent. By use of eqs 1 and 2, these can be converted to third-order susceptibilities $\chi^{(3)}$. We then assume the solute and solvent properties are additive so that

$$\chi^{(3)}_{solution} = (1 - f)\chi^{(3)}_{solvent} + f\chi^{(3)}_{solute} \tag{3}$$

Equation 3 is assumed to be valid for both the real and imaginary parts of $\chi^{(3)}$. Using eq 3, we can determine $\chi^{(3)}$ for the solute.

To compare one molecular species to another, it is convenient to define molecular nonlinear properties, termed molecular hyperpolarizabilities γ. The real and imaginary parts, γ_R and γ_I, characterize the nonlinear refraction and nonlinear absorption, respectively. The real part γ_R is given by

$$\gamma_R = \frac{\chi_R^{(3)}}{L^4 N} \tag{4}$$

and the imaginary part γ_I by

$$\gamma_I = \frac{\chi_I^{(3)}}{L^4 N} \tag{5}$$

where L is the Lorenz correction factor,[13] $L = (n_0{}^2 + 2)/3$, and N is the number density.

It is useful to have figures of merit that combine the nonlinear susceptibility and the linear or nonlinear absorption, referred to as W/I_0 and T^{-1}, respectively.[14] For almost any practical material, the linear absorption coefficient, α_0, must be small. More transparent materials will therefore have larger values of the figure of merit W/I_0, defined as

$$\frac{W}{I_0} = \frac{n_2^I}{\alpha_0 \lambda} \tag{6}$$

At the large intensities needed to operate nonlinear optical devices, the nonlinear absorption must be small as well. This requirement is expressed as the figure of merit T^{-1},

$$T^{-1} = \frac{n_2^I}{2\lambda\alpha_2} \tag{7}$$

T^{-1} is larger for materials with smaller nonlinear absorption.

Experimental Section

Synthesis. Syntheses employed standard Schlenk techniques, but workups were conducted in air. Unless noted otherwise, reagents and solvents were used as purchased. The heterocyclic compounds, C_3S_7O and $C_6S_6O_2$, were prepared according to literature methods[15] starting from $(Bu_4N)_2[Zn(C_3S_5)_2]$.[16] The zinc clusters, $(Me_4N)_2[Zn_4(SPh)_6]$ and $(Me_4N)_4[Zn_{10}S_4(SPh)_{16}]$, were synthesized according to Dance's methods.[17] *n*-Butylferrocene (*n*-BuFc) was purchased from Aldrich and used as received. The *n*-butylferrocene disulfide polymer $(BuFcS_2)_n$ was made from *n*-BuFc according to a literature procedure.[18]

Synthesis of α-$C_3S_3(SCH_2Ph)_2$.[19] This species was prepared by treating a solution of $(Bu_4N)_2[Zn(\alpha\text{-}C_3S_5)_2]$ (1.06 g, 1.12 mmol) in 30 mL of acetone with benzyl chloride (0.78 mL, 6.78 mmol) and stirring it for 16 h at room temperature, during which time the solution turned from deep purple to orange. To isolate the compound, the orange solution was concentrated under reduced pressure until a precipitate began to form; the resulting mixture was then diluted with an approximately equal volume of 2-propanol. Further concentration yielded α-$C_3S_3(SCH_2Ph)_2$ in the form of yellow crystals (0.70 g, 82%).

Synthesis of β-$C_3S_3(SCH_2Ph)_2$.[20] To a 2.0 M solution of sodium methoxide in methanol (16.5 mL) was added β-$C_3S_5(COPh)_2$[20] (2.24 g, 5.52 mmol), and the resulting brown mixture was stirred at ambient temperature. Ammonium acetate (2.8 g) was added, and the mixture was diluted with water, resulting in a red solution. A solution of benzyl chloride (0.650 mL, 5.65 mmol) in methanol (14 mL) was added dropwise over 15 min, during which time a yellow, crystalline solid formed. This was collected by filtration, washed with water, and dried in vacuo (0.62 g, 30%). Anal. Calcd for $C_{17}H_{14}S_5$: C, 53.93; H, 3.73. Found: C, 53.53; H, 3.91. ^{1}H NMR (CD_3COCD_3, 500 MHz): δ 4.12 (s, 2H), 4.49 (s, 2H), 7.24 (m, 5H), 7.37 (m, 5H).

Synthesis of $C_6S_8O_2$. A slurry of C_6S_{10}[21] (2.83 g, 7.22 mmol) in chloroform (100 mL) was treated with a slurry of 9.19 g (28.8 mmol) of mercuric acetate in glacial acetic acid (60 mL). The orange suspension was heated to reflux for 17 h and allowed to cool to ambient temperature, and a brown solid was removed by filtration, leaving a yellow solution. This was washed twice with water (0.1 L portions), then with 0.1 L of 3% aqueous sodium carbonate, then again with two 0.1 L portions of water. The organic fraction was dried over magnesium sulfate and concentrated to half its volume. The golden solution was diluted with an equal volume of isopropyl alcohol and concentrated until yellow crystals (0.136 g, 5.2%) formed. IR (KBr): 1722 (w), 1662 (s, ν_{C-O}), 1588 (sh), 996 (w), 872 (w), 734 (w), 420 (w) cm^{-1}.

Synthesis of $(Me_4N)_2[Cu_4(SPh)_6]$. This compound was synthesized by adapting Dance's procedure.[22] A 500 mL flask was charged with 250 mL of oxygen-free ethanol followed by 4.00 g (25.9 mmol) of Me_4NBr, 5.60 mL (54.5 mmol) of benzenethiol, and 6.90 mL (49.5 mmol) of Et_3N. The mixture was stirred and heated at reflux for 30 min at which stage most of the quaternary ammonium salt dissolved. After allowing the mixture to cool to ca. 50 °C, the reaction solution was treated with a solution of 2.90 g (12.5 mmol) $Cu(NO_3)_2 \cdot 2.5H_2O$ in 50 mL of oxygen-free ethanol over a course of 15 min. The resulting pale-yellow, turbid mixture was reheated to the boiling point and diluted with 40 mL of acetonitrile to partially dissolve the precipitate. The mixture was allowed to cool to room temperature. After the slurry stood undisturbed for 10 h, pale-yellow flakes were collected by filtration in an oxygen-free atmosphere, washed with 20 mL of water and 20 mL of methanol, and dried in vacuo. Yield: 2.45 g (74% based on copper). Anal. Calcd for $C_{44}H_{54}N_2Cu_4S_6$: C, 49.97; H, 5.15; N, 2.65. Found: C, 49.74; H, 5.20; N, 2.51. The bright-yellow pentacopper cluster, $(Me_4N)_2[Cu_5(SPh)_7]$,[22] can be converted to $(Me_4N)_2[Cu_4(SPh)_6]$ using the following procedure. $(Me_4N)_2[Cu_5(SPh)_7]$ (0.264 g, 0.214 mmol) was treated with acetonitrile (60 mL), resulting in a yellow solution and some undissolved solid. Me_4NBr (0.360 g, 2.34 mmol) and thiophenol (0.22 mL, 2.1 mmol) were added. The mixture was then treated with triethylamine (0.5 mL), whereupon the remaining yellow solid dissolved immediately, the yellow color of the solution became much paler, and some white solid precipitated. The mixture was then diluted with 2-propanol (60 mL), stirred until the white solid redissolved (20 min), and concentrated until the liquid became slightly turbid. The mixture was sealed and allowed to stand for 72 h, at which time pale-yellow crystals formed (0.150 g, 53% based on copper).

***Z*-Scan Technique.** Fundamentals of the *Z*-scan technique have been discussed elsewhere,[12] and so only a brief description is given here. Figure 1 shows the experimental setup. A diode-pumped mode-locked Nd^{3+}:YLiF (YLF) oscillator generates a ~20 ps, 1.053 μm pulse, which is injected in a YLF regenerative amplifier. The amplifier is cavity-dumped at a rate of 640 Hz. This continuously pumped YLF amplifier produces a high-quality beam with a single transverse mode Gaussian (TEM_{00}) profile. The cavity-dumped pulse of ~800 μJ energy is frequency-doubled to $\lambda = 527$ nm. The duration of the 527 nm pulse is 27 ± 2 ps. The pulse energy could be continuously varied using a half-wave plate and a polarizing beam splitter.

In the *Z*-scan apparatus, the pulse is focused into a sample, which is translated along the axis of pulse propagation (the *Z*-axis). Three solid-state detectors are used. A portion of the incoming pulse is split off into D3 (ThorLabs DET2-SI), which is used to normalize for intensity fluctuations. The pulse

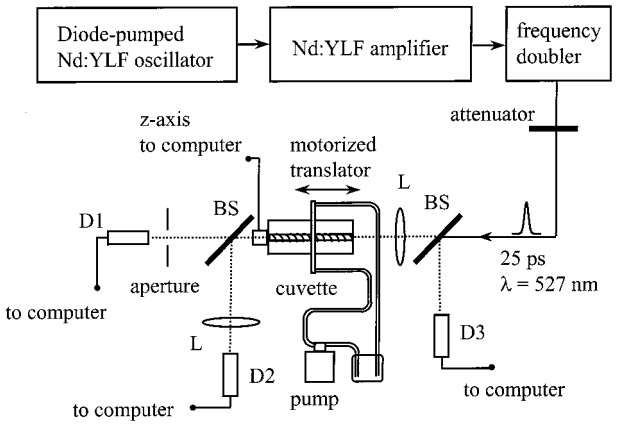

Figure 1. Apparatus used for *Z*-scan measurements. Key: BS = beam splitter; L = lens; D = silicon photodetector.

transmitted through the sample is split into two parts. One part, which generates the "open-aperture" data, is focused onto D2 (ThorLabs DET1-SI) with a lens. As the sample moves in and out of the focus, nonlinear absorption causes the intensity seen by D2 to vary. Nonlinear refraction (due to the real part of the nonlinear susceptibility) has no effect on the signal seen by D2. The second part, which generates the "closed-aperture" data, goes through a 1.5 mm aperture in the far field before reaching D1 (ThorLabs DET1-SI). As the sample moves in and out of the focus, both nonlinear refraction and nonlinear absorption effects cause the pulse diameter in the far field to vary. The aperture converts this diameter variation into an intensity variation detected by D1.

In our setup, a solution is pumped through an optical cell (Uvonic 1 mm, type 48) at a velocity that ensured that a fresh volume is irradiated by each succeeding pulse. That occurs when the linear flow velocity v is much greater than dF, where d is the Gaussian beam diameter and F the laser repetition rate. For a diameter $d = 40$ μm and a repetition rate $F = 640$ s^{-1}, the velocity should exceed 2.5 cm s^{-1}. The actual linear flow velocity used was $v = 25$ cm s^{-1}. In this manner, we measured the fast electronic and rotational contributions while eliminating undesirable cumulative effects such as thermal lensing. The cell is mounted on a motorized translation stage with a location sensor. A computer, with an analog-to-digital converter, samples the output of the three detectors and the location sensor.

The intensity of the laser pulse at the focus in air is computed knowing the energy, the Gaussian beam radius ($r_0 = 20.0 \pm 3$ μm), and the pulse duration ($t_p = 27$ ps). Gaussian beam radius denotes the $1/e^2$ intensity point. These parameters were determined with a pulse energy meter, a knife-edge beam profile measurement, and background-free autocorrelation. For each sample, we obtained data on a dilute solution and on the pure solvent. Data were taken at two intensities, 1.3 ± 0.2 and 3.6 ± 0.2 μJ, corresponding to peak intensities of 16 and 43 GW/cm^2. With the lower value, nonlinear effects are reduced in magnitude, but any effects caused by optical inhomogeneities in the moving cuvette remain, allowing the data to be corrected for such effects.

The *Z*-scan analytical functions have been thoroughly detailed elsewhere. We used the thin-sample analysis functions derived by Sheik-Bahae et al.[12] The thin-sample approximation is derived in the limit where the Rayleigh range exceeds the sample thickness. Here, the Rayleigh range in air is 2.4 mm and the sample thickness is 1 mm. In ref 12, it is shown that the distance between the peaks and valleys of the closed-aperture scan should be about 1.7 times the Rayleigh range. That would mean a peak-

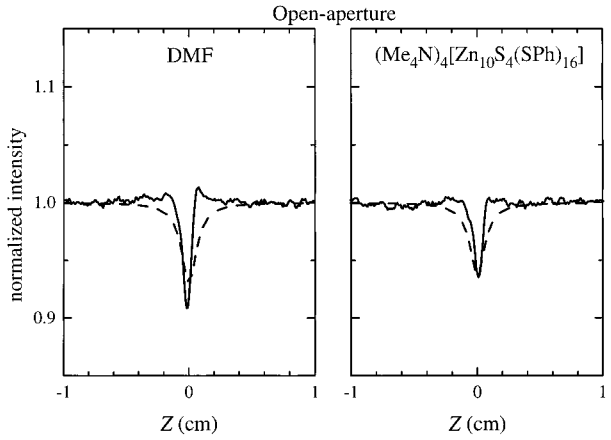

Figure 2. Open-aperture data for pure dimethylformamide (DMF) and a DMF solution of $(Me_4N)_4[Zn_{10}S_4(SPh)_{16}]$. The dashed curves are theoretical fits using the thin-sample functions of Sheik-Bahae et al. (ref 12).

to-valley distance of about 4 mm in our experimental data. If the peak-to-valley distance is significantly different, there would be two likely possibilities. If the sample were too thick, the *Z*-scan data would take on a distinctive shape. There would be a characteristic flat region around the focus at $Z = 0$,[23] and the peak-to-valley separation would become greater than predicted by the thin-sample model, by an amount that increases with increasing sample thickness (for example, see Figure 2 of ref 23). The other possibility is self-focusing. As discussed in detail by Hughes et al.,[24] significant self-focusing effects on *Z*-scan data have been previously observed in thin samples with pulses (15 ps duration, 532 nm) similar to those used here. If self-focusing were to occur in the sample, the effective Rayleigh range would be decreased. The peak-to-valley distance would then become smaller than predicted by the thin-sample model. In that case, following a suggestion from Sheikh-Bahae et al.,[12] an approximate correction for self-focusing can be obtained by allowing the Rayleigh range to vary. In general, our data do not show the characteristic flat region indicating a thick sample, but they do show peak-to-valley separations that are somewhat less than predicted by the thin-sample treatment. That indicates significant effects from self-focusing, so we allowed the Rayleigh range to vary in fitting the data. To verify that no significant errors were introduced by using the thin-sample approximation, some of the data were fit using the full thick-sample treatment,[25] which produced results that were always identical to those obtained with the thin-sample approximation.

Results

We first discuss in detail how measurements are made and interpreted for a specific example, the sulfur-rich compound $(Me_4N)_4[Zn_{10}S_4(SPh)_{16}]$, and then cite results for other compounds in Tables 1−3. We chose *N*,*N*-dimethylformamide (DMF) as the solvent for $(Me_4N)_4[Zn_{10}S_4(SPh)_{16}]$. First, measurements were made on pure DMF, which, like the other solvents discussed in this work, is colorless, i.e., $\alpha_0 = 0$. The data for pure DMF are shown in Figures 2 and 3.

In Figure 2, there is a dip in the signal near the focus at $Z = 0$ where the intensity is at a maximum. This dip indicates reduced transmission of 527 nm pulses near the focus, caused by nonlinear absorption. The value of the nonlinear absorption coefficient was determined as discussed above, by fitting the data to the open-aperture transmission function of Sheik-Bahae et al.,[12] with the Rayleigh range and the nonlinear absorption coefficient α_2 as free parameters. The result for pure DMF at 527 nm was $\alpha_2 = 1.4 \times 10^{-11}$ m W^{-1}. The dashed curve in the left-hand graph of Figure 2 is the theoretical fit. The difference between the data and the fitted curve is attributed to the somewhat too-simple treatment of the self-focusing, which in a full treatment should be considered to vary as the cell moves through the beam waist as in the beam propagation methods discussed in ref 24. In the closed-aperture data, shown in Figure 3, a dip for $Z < 0$ and a peak for $Z > 0$ are observed. This behavior is indicative of a nonlinear lens with a positive value of n_2^I. When the data were fit to the closed-aperture transmission function (dashed curve in Figure 3) using the above values of α_2 and the Rayleigh range, while varying n_2^I, the value $n_2^I = 8.3 \times 10^{-19}$ m^2 W^{-1} was obtained (see Table 1).

When the measurements of pure DMF were completed, a solution of $(Me_4N)_4[Zn_{10}S_4(SPh)_{16}]$ (0.809 mM) in DMF was studied. The solution had no detectable absorbance at 527 nm, so $\alpha_0 = 0$. The open-aperture data (Figure 2) are indistinguishable from pure DMF, indicating that α_2 for the solute alone was essentially zero. In the closed-aperture configuration in solution (Figure 3), there is a peak at $Z < 0$ and a dip at $Z > 0$. These features indicate that the nonlinear refraction of the solution is greater than and opposite in sign from that of the solvent. The value of n_2^I could then be varied to fit the solution data, as shown in Figure 3.

To obtain the properties for the solute alone, we use eq 3. We could convert the above α_2 and n_2^I measurements into $\chi^{(3)}$ and plug them into eq 3. However, since the theoretical curves do not exactly fit the pure solvent data, we used another procedure that we believe is more accurate and not dependent on how the pure solvent data are interpreted. We simply subtracted the closed-aperture and open-aperture data for the pure solvent from the solution data. We then fit the difference data as above to obtain the solute's contribution to α_2 and n_2^I. We obtained the value $n_2^I = -1.3 \times 10^{-18}$ m^2 W^{-1} for $(Me_4N)_4[Zn_{10}S_4(SPh)_{16}]$. We then computed molecular hyperpolarizabilities γ_R and γ_I given in Table 2 using eqs 4 and 5 and figures of merit W and T^{-1} using eqs 6 and 7.

We also measured the NLO properties of several common solvents, which are given in Table 1. Table 2 presents results for 12 sulfur-rich molecules (plus CS_2). For the *n*-butylferrocene persulfide polymer, the mole fraction *f* in eq 3 was calculated as the mole fraction of the monomer. Table 3 lists the figures of merit W/I_0 and T^{-1} for the sulfur-rich molecules examined in this work.

Discussion

The structures of some of the sulfur-rich molecule are shown in Figure 4. They fall into five categories: (1) molecular sulfur, (2) derivatives of the isomers of $C_3S_5^{2-}$, (3) a series of C_3S_5-derived dithiocarbonates, (4) ferrocenes, and (5) metal sulfido clusters. All the solutions were either colorless or yellow. The yellow solutions had some linear absorption at 527 nm, which resulted in a depressed figure-of-merit W/I_0 (Table 3).

Solvents. Both CS_2 and toluene have been studied extensively and are used as standards to test the accuracy of our absolute measurements.[5,12,23] For CS_2, we found $n_2^I = 3.0 \times 10^{-18}$ m^2 W^{-1} at 527 nm and 27 ps. Converting into units used by other authors, we obtain a nonlinear refractive index $n_2 = 1.16 \times 10^{-11}$ esu (the conversion is $n_2 = n_0 c n_2^I/(40\pi)$). Other authors working at $\lambda = 532$ nm and 30 ps report $n_2 = 1.2 \times 10^{-11}$ esu[12] and 1.05×10^{-11} esu,[26] in good agreement with our results. For toluene, we found $n_2^I = 9.5 \times 10^{-19}$ m^2 W^{-1} at 527 nm and 27 ps, which converts to $n_2 = 3.3 \times 10^{-12}$ esu. Other

TABLE 1: Nonlinear Properties at $\lambda = 527$ nm of Solvents Used in This Work

solvent	concn (M)	N (10^{24} m^{-3})	n_0	n_2^I (10^{-18} m^2 W^{-1})	$\chi_R^{(3)}$ (10^{-33} C m V^{-3})	γ_R (10^{-57} C m^4 V^{-3})	α_2 (10^{-12} m W^{-1})	$\chi_I^{(3)}$ (10^{-33} C m V^{-3})	γ_I (10^{-57} C m^4 V^{-3})
CS_2	16.63	10015	1.627	3.0 ± 0.1	370	0.0065	0.8	84	0.0015
toluene	9.39	5650	1.4960	0.93	98	0.0043	2.7	240	0.0106
CH_2Cl_2[a]	15.60	9390	1.4240	−0.44	−43	−0.0014	0.2	16	0.00052
CH_3CN	19.15	11530	1.3440	−0.27	−23	−0.00077	0.3	21	0.00071
DMF	12.91	7774	1.4310	0.83	80	0.0031	14	1100	0.044

[a] Value obtained with lower intensity (1.3 μJ pulses). With higher intensity pulses, a positive component to the nonlinear refraction was also observed.

TABLE 2: Nonlinear Optical Properties at $\lambda = 527$ nm of Sulfur-Rich Molecules

molecular species	solvent	concn (mM)	N (10^{24} m^{-3})	n_0	n_2^I (10^{-18} m^2 W^{-1})	$\chi_R^{(3)}$ (10^{-33} C m V^{-3})	γ_R (10^{-57} C m^4 V^{-3})	α_2 (10^{-12} m W^{-1})	$\chi_I^{(3)}$ (10^{-33} C m V^{-3})	γ_I (10^{-57} C m^4 V^{-3})	α_0 (m^{-1})
CS_2	neat	16630	10015	1.627	3.0 ± 0.1	370	0.0065	0.8	84	0.0015	0
S_8	toluene	21.0	12.6	1.4960	-0.25 ± 0.02	−26	−0.52	0.2 ± 0.2	18	0.35	0
α-$C_3S_3(SCH_2Ph)_2$	CH_2Cl_2	7.01	4.22	1.4240	-0.15 ± 0.02	−14	−1.04	7.9 ± 0.2	630	46	10.9
β-$C_3S_3(SCH_2Ph)_2$	CH_2Cl_2	7.01	4.22	1.4240	-0.93 ± 0.02	−89	−6.5	4.0 ± 0.2	320	23	76.5
C_3S_7O	CH_2Cl_2	10.0	6.02	1.4240	−(<0.1)	−(<10)	−(<0.5)	0.5 ± 0.2	40	2	2
$C_6S_6O_2$	CH_2Cl_2	1.09	0.656	1.4240	-1.36 ± 0.1	−130	−60.8	0.8 ± 0.2	64	30	5.6
$C_6S_8O_2$	CH_2Cl_2	1.88	1.132	1.4240	-1.05 ± 0.1	−100	−27.2	0.0 ± 0.2	±(<16)	±(<4)	4.6
BuFc	CH_2Cl_2	11.3	6.80	1.4240	−0.79	−75	−3.4	2.1 ± 0.2	170	7.6	18
$(BuFcS_2)_n$	CH_2Cl_2	11.26	6.781	1.4240	3.6 ± 0.2	340	15.6	18.2 ± 0.5	1460	66	201
$(Me_4N)_2[Cu_4(SPh)_6]$	CH_3CN	5.48	3.30	1.3440	-0.13 ± 0.02	−11	−1.3	0.0 ± 0.2	±(<15)	±(<2)	44
ZnS_6(TMEDA)	CH_2Cl_2	4.24	2.55	1.4240	−(<0.1)	−(<10)	−(<1)	0.0 ± 0.2	±(<16)	±(<2)	1.3
$(Me_4N)_2[Zn_4(SPh)_{10}]$	CH_3CN	5.04	3.04	1.3440	0.38 ± 0.02	32	4.1	0.8 ± 0.2	57	7.2	0
$(Me_4N)_4[Zn_{10}S_4(SPh)_{16}]$	DMF	0.809	0.487	1.4310	-1.3 ± 0.1	−130	−78	0.0 ± 0.2	±(<16)	±(<10)	0

TABLE 3: Figures of Merit at 527 nm for Sulfur-Rich Molecules

molecular species	$\lvert W\rvert/I_0$ 10^{-15} m^2 W^{-1}	$\lvert T\rvert^{-1}$
CS_2	large	3.6
S_8	large	>1.2
α-$C_3S_3(SCH_2Ph)_2$	26	0.02
β-$C_3S_3(SCH_2Ph)_2$	23	0.22
C_3S_7O	<100	<0.2
$C_6S_6O_2$	460	1.6
$C_6S_8O_2$	430	>5
$(BuFcS_2)_n$	34	0.19
BuFc	83	0.36
$(Me_4N)_2[Cu_4(SPh)_6]$	6	>0.6
ZnS_6(TMEDA)	<150	very large
$(Me_4N)_2[Zn_4(SPh)_{10}]$	large	0.5
$(Me_4N)_4[Zn_{10}S_4(SPh)_{16}]$	large	>6.2

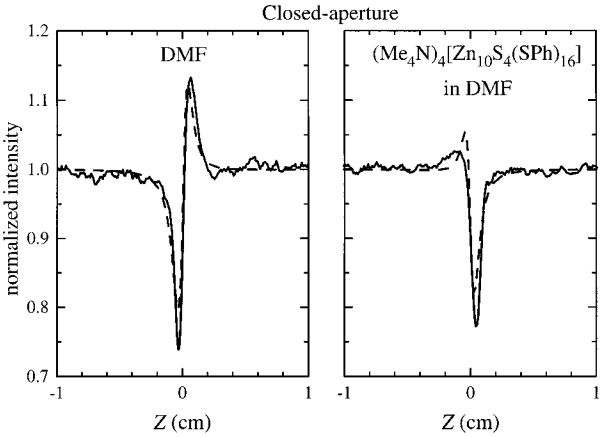

Figure 3. Closed-aperture data for pure dimethylformamide (DMF) and a solution of $(Me_4N)_4[Zn_{10}S_4(SPh)_{16}]$. The dashed curves are theoretical fits using the thin-sample functions of Sheik-Bahae et al. (ref 12).

authors have reported 6×10^{-12} esu at 532 nm and 25 ps, which is within a factor of 2 of our measurement.[24] Some of this difference may be attributed to experimental errors and some to impurities in the toluene.

Some interesting results were obtained with CH_2Cl_2. The nonlinear parameters were intensity-dependent. At lower intensity, the nonlinear refraction was relatively small and it had a negative sign, which is unusual for a colorless solvent. At higher intensity, a larger positive nonlinearity was observed. The values for CH_2Cl_2 cited in Table 1 were obtained with lower intensity pulses. A negative nonlinear refractive index is usually associated with the presence of nearby electronic states. For example, CH_2Cl_2 has some low-lying electronic states near 450 nm. We can speculate that the negative nonlinear refraction might be associated with the tail of this transition or with a transition involving two photons at 527 nm or possibly due to stabilizers or impurities in the solvent. Acetonitrile also showed negative nonlinear refraction, which was very small. Since acetonitrile's electronic excited states are deep in the ultraviolet, this small negative nonlinearity might well be due to impurities.

It should be emphasized that the determination of nonlinear parameters for the neat solvents themselves has no effect on our determination of nonlinear parameters for the sulfur-containing molecules because in our method we simply subtract the neat solvent data from the dilute solution data.[8,12] However, two points are worth mentioning about this method. First, the results may be solvent-dependent; this effect would be quite severe to the extent that the degree of aggregation, solvation, or protonation is affected. Such complications are negligible for our samples, the solution properties of which are normal. Second, nonlinear properties of solutes are best obtained when the solvent contributes less to the nonlinear refraction and absorption than does the solute. As shown in Table 1, acetonitrile and dichloromethane are the best solvents in this regard and CS_2 is the worst.

Whereas our approach is the simplest way of screening many different materials, once an interesting material is found, more extensive studies should be performed. These might include concentration dependence, wavelength dependence, and pulse-width dependence. Concentration dependence could be espe-

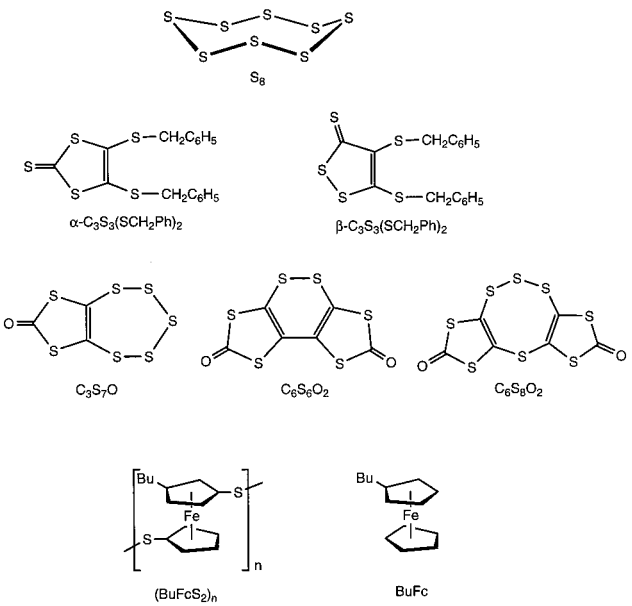

Figure 4. Structures of some of the sulfur-rich molecules studied in this work.

SCHEME 1

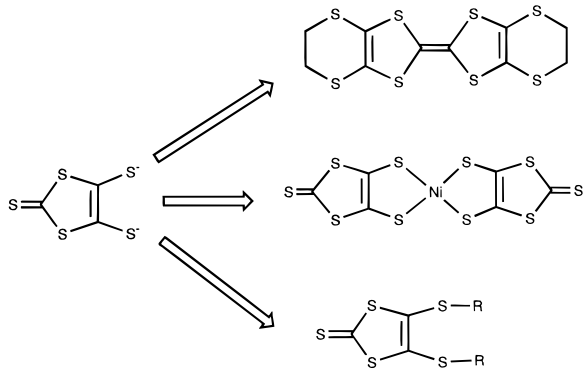

cially useful because it might provide insights into how the solute would perform in the solid state. Furthermore, at high solute concentrations, solute−solute interactions could slow molecular reorientation. Of course, in the limiting case of a solid, molecular reorientation is totally suppressed and the intrinsic electronic and nuclear hyperpolarizabilities dominate.

Sulfur. Given that this project focused on sulfur-rich molecules, it seemed worthwhile to study sulfur itself. Elemental sulfur exists in a number of allotropes, the most common being S_8. It is known, however, that in solution, S_8 exists in equilibrium with small amounts of other cyclic species, such as S_7.[27] Toluene solutions of S_8 were found to have no measurable linear or nonlinear absorption at 527 nm. The γ_R value of S_8 is about 80 times larger than CS_2 and opposite in sign. Thus, on a molecule-to-molecule basis, S_8 is superior to CS_2 in its nonlinear properties. Of course, we are ultimately comparing pure liquid CS_2, where one has an extremely large number density of small molecules that rotate quickly, to a dilute solution of S_8. In future work, it would be interesting to compare the bulk nonlinear parameters of liquid CS_2 to crystalline S_8.

Derivatives of $C_3S_5^{2-}$. Anions of the formula $C_3S_5^{2-}$ have attracted much attention in the materials science community because they are widely employed as precursors to two major classes of electronic materials, metal dithiolenes and tetrathiafulvalenes (Scheme 1).[28] Recent work has shown that transition metal derivatives of C_3S_5 exhibit high nonlinear refraction as well.[10,29] Given the intense interest in these materials, we investigated the nonlinear refractive properties of the core heterocycle. Two isomers of $C_3S_5^{2-}$ are known. The great majority of previous studies has focused on the α isomer (see Scheme 1 and Figure 4), also known as dmit. A second, thermodynamically more stable β isomer of $C_3S_5^{2-}$ is also known, wherein the three carbon atoms are adjacent. For this study we prepared the dibenzyl derivative of both isomers of $C_3S_5^{2-}$, i.e., α- and β-$C_3S_3(SCH_2Ph)_2$. These neutral dibenzyl compounds have high solubility in nonpolar solvents.

Both the α and β isomers of $C_3S_3(SCH_2Ph)_2$ have absorptions at 527 nm, with linear absorption coefficients of $\alpha_0 = 10.9$ and 76.5 m^{-1}, respectively. (Note that these linear absorption values are concentration-dependent and are reported for the concentrations used in the *z*-scan measurements; the extinction coefficients for the α and β isomers are 15.5 and 109 M^{-1} cm^{-1}, respectively.) The open-aperture measurements show that both species exhibit substantial nonlinear absorption. The nonlinear refraction for the β isomer is greater than that of the α isomer. It is difficult to rationalize the differing hyperpolarizability values for the C_3S_5 ring compounds except to note that the β isomer is a better Bronsted base; this might suggest that it is more polarizable. To some extent their linear absorption coefficients precludes further interest on our part. However, the α isomer is a useful reference material because the core is easily functionalized at the terminal thiolato groups (Scheme 1); this versatility might make it possible to optimize or fine-tune optical and processing properties. Additionally, as discussed in the next section, some of its derivatives may exhibit both substantial second hyperpolarizabilities as well as low linear absorption coefficients.

Dithiocarbonates. We evaluated a recently synthesized series[15,21] of dithiocarbonates, which are derived from the α isomer of C_3S_5. These compounds exhibit extended structures (bicyclic or tricyclic) that should enhance their polarizabilities (and therefore their γ_R values). Three dithiocarbonates were examined: the bicyclic species C_3S_7O, which contains a polysulfur chain-linked to the dithiocarbonate, and two tricyclic species $C_6S_6O_2$ and $C_6S_8O_2$, which feature two dithiocarbonates attached to C_4S_2 and C_4S_4 cores, respectively (see Figure 4). The α isomer of C_3S_5 is a trithiocarbonate (i.e., bearing the functionality $(RS)_2C{=}S$); we made the dithiocarbonate by substituting an oxygen atom for the terminal sulfur. This was done because the tricyclic trithiocarbonates, C_6S_8 and C_6S_{10}, are nearly insoluble; C_6S_8 is only slightly soluble in CH_2Cl_2, and C_6S_{10} is soluble (slightly) only in CS_2. Additionally, it is known that carbonyls have a larger HOMO−LUMO gap than thiocarbonyls;[30] this could be expected to result in a lower linear absorption in the visible spectrum. Therefore, the dithiocarbonates could exhibit a larger nonlinear refraction due to the increased conjugation, without a correspondingly larger linear absorbance.

Consistent with the expected influence of the oxygen vs the sulfur on the energy of the associated n to π^* transition, C_3S_7O did indeed exhibit a diminished extinction coefficient (2 M^{-1} cm^{-1}, with an absorption coefficient of 2 m^{-1} at the concentration used) compared to the $C_3S_3(SCH_2Ph)_2$ isomers. On the other hand, the two tricyclic molecules, $C_6S_6O_2$ and $C_6S_8O_2$, had extinction coefficients at 527 nm of 51 and 24.5 M^{-1} cm^{-1}, which were between those of the α and β isomers of C_3S_3-$(SCH_2Ph)_2$. (The small linear absorption coefficients, 5.6 and 4.6 m^{-1}, respectively, are due to the lower concentrations used). However, $C_6S_6O_2$ and $C_6S_8O_2$ have much larger γ_R values (-6.08×10^{-56} and -2.72×10^{-56} C m^4 V^{-3}, respectively) than the $C_3S_3(SCH_2Ph)_2$ isomers. The nonlinear absorption

CHART 1

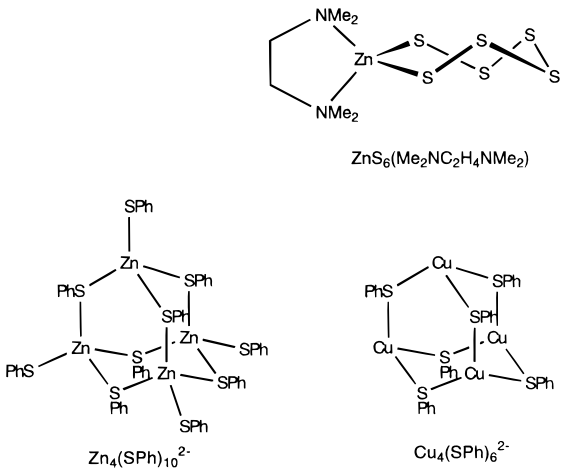

coefficients are modest for two of these species, C_3S_7O and $C_6S_8O_2$. For $C_6S_6O_2$, however, γ_I is large and comparable to those seen for the C_3S_5 derivatives; the corresponding figure of merit, T^{-1}, reflects this deficiency. It is also interesting to compare the effect of cumulated S−S bonds, cf. S_8, vs the effect of cumulated C_2S_2CO rings; the monodithiocarbonate displays only a modest nonlinear refraction.

Ferrocenes. Ferrocenes have been examined as candidates for photonic materials because of the discovery of high first hyperpolarizabilities for ferrocene-substituted olefins by Marder, Green, and their co-workers.[31] Ferrocenes are effective donors in push−pull $\chi^{(2)}$ molecules. In the present context, ferrocenes are of interest in view of the recent synthesis of ferrocene persulfide (S−S) polymer (Figure 4). Electrochemical measurements indicate that the subunits in these polymers are strongly coupled.[32] This coupling implies a delocalized ground state,[33] hence, the potential for a large value of γ_R.

Our results show that the sulfur-linked ferrocenes indeed exhibit higher nonlinear refraction than ferrocene itself. The polymers, however, suffer from substantial linear and nonlinear absorption. In terms of the figures of merit in Table 3, the absorption effects offset the benefits of the enhanced γ_R.

Small Metal Sulfido Ensembles. Recent work has shown that metal sulfido clusters display substantial nonlinear refraction and nonlinear absorption.[34] It appears that most such systems have substantial linear absorption properties,[35] and we were interested in examining species without this detracting feature. A series of three species were selected for this part of the study (Chart 1). As a reference compound, we started with the simple complex ZnS_6(TMEDA). In this compound the S_6^{2-} chain is bound at its termini to the tetrahedral Zn^{2+} center, whose other two coordination sites are occupied by tetramethylethylenediamine (TMEDA).[36] We examined two thiolato clusters, $Zn_4(SPh)_{10}^{2-}$ and $Cu_4(SPh)_6^{2-}$. Despite their structural complexity, these species are easily synthesized by high-yielding reactions from simple reagents. Both clusters feature tetrahedral arrays of d^{10} metal centers (Cu^+, Zn^{2+}). The zinc species has both bridging and terminal thiolato ligands, whereas in the copper clusters, the thiolates are bridging. The copper thiolato cluster had been previously examined where it was claimed to exhibit one of the highest values of γ_R for a transition metal complex. We were interested in reconfirming this observation at shorter pulse widths and comparing these results with the Zn_4 species. The Zn_4 cluster is very robust and, relative to the Cu_4 species, has improved linear optical properties relative to the Cu_4 species.

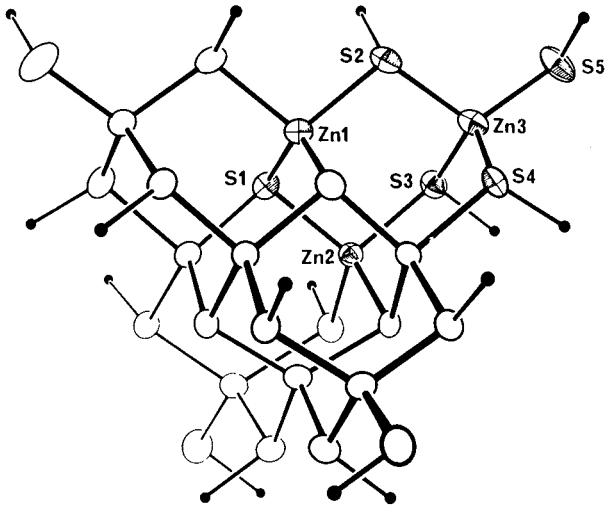

Figure 5. Structure of the $[Zn_{10}S_4(SPh)_{16}]^{4-}$ anion, taken from ref 17.

Starting with ZnS_6(TMEDA), the linear absorption, which is weak, is attributed to a ligand (sulfido) to metal charge transfer band centered in the UV. This species displays only a modest γ_R, reminiscent of the results for other polysulfide molecules, such as C_3S_7O and S_8 (see above). On the other hand, the tetrazinc species $(Me_4N)_2[Zn_4(SPh)_{10}]$ has a sizable γ_R value. Despite a modest linear absorption, the encouraging nonlinear refraction data were offset somewhat by nonlinear absorption effects. We now turn to the copper cluster $Cu_4(SPh)_6^{2-}$, which Shi and co-workers[33] have reported to exhibit an "extraordinary" second hyperpolarizability. As implied by Dance et al.,[22] this Cu_4 cluster is chemically labile in solution; bright-yellow crystals of the pentacopper cluster, $Cu_5(SPh)_7^{2-}$, often form along with (or instead of) $Cu_4(SPh)_6^{2-}$, which crystallizes in the form of pale-yellow flakes (see Experimental Section). In view of this complication, it is likely that both this and Shi et al.'s studies were conducted on a mixture of the Cu_4 and Cu_5 clusters. We confirmed, however, that these samples suffer a substantial linear absorption.

Studies on $Zn_{10}S_4(SPh)_{16}^{4-}$. We derived two conclusions based on the experiments described in the previous section: (i) these metal clusters exhibit higher optical nonlinearities than mononuclear complexes and (ii) the undesirable absorption characteristics of the Cu_4 cluster were not exhibited by the Zn_4 analogue. These results encouraged us to extend the series to include the still larger cluster $[Zn_{10}S_4(SPh)_{16}]$,[4−17,37] the structure of which is depicted in Figure 5. This colorless anion was studied as its tetramethylammonium salt, which confers solubility in DMF. Like the Zn_4 cluster, the Zn_{10} compound exhibits no linear absorption. Furthermore, it displays virtually no nonlinear absorption. Its second hyperpolarizability is the greatest of the series of compounds studied in this work. The favorable juxtaposition of absorption and refraction properties is reflected in the exceptional figures of merit (Table 3).

Conclusion

In this work we have examined the nonlinear absorption and nonlinear refraction of solutions of a series of sulfur-rich molecules and anions. Molecular properties γ_R and γ_I were extracted by subtracting the contribution from the solvent. This study represents a quantitative evaluation of the qualitative idea that species containing large numbers of the highly polarizable sulfur centers would exhibit large nonlinear refraction in the absence of significant linear or nonlinear absorption. This hypothesis is confirmed. The accumulation of a large number

of S atoms does not, by itself, give rise to optimal properties; rather, the electronic polarizability correlates with the number of sulfido (S^{2-}) centers. Our survey identified two structural families with particularly promising optical properties, the Zn−S−SPh clusters and the condensed dithiocarbonates. In both cases the greatest figures of merit were obtained for the largest molecules. Further synthetic work is planned to develop related structures with still more extended structures.

Previous work on the second hyperpolarizability of sulfur-rich compounds examined only species with substantial linear absorption coefficients. The present work shows that high figures of merit can be achieved without the undesirable effects of linear absorption.

Acknowledgment. This work was supported by grants from the Department of Energy, DOE DEFG (T.B.R.) through the Seitz Materials Research Laboratory, the National Science Foundation, DMR 97-14843 (D.D.D.), and a contract from the Air Force Office of Scientific Research, F4960-97-1-0056 (D.D.D.). L.K.I. acknowledges support from the AASERT program, sponsored by the U.S. Army Research Office, Contract DAAG55-98-1-0191. We thank one referee for insightful comments and criticisms.

References and Notes

(1) *Nonlinear Optics of Organic Molecules and Polymers*; Narwa, N. S., Miyata, S., Eds.; CRC Press: Tokyo, 1996.
(2) Clymer, B.; Collins, S. A. *Opt. Eng.* **1985**, *24*, 74.
(3) Mizrahi, V.; DeLong, K. W.; Stegemann, G. I. *Opt. Lett.* **1990**, *14*, 1140.
(4) Natarajan, L. V.; Sutherland, R. L.; Tondiglia, V. P.; Bunning, T. J.; Adams, W. W. *J. Nonlinear Opt. Phys. Mater.* **1996**, *5*, 89−98. (b) Tang, N.; Su, W.; Cooper, T.; Adams, W.; Brandelik, D.; Brant, M.; McLean, D.; Sutherland, R. *SPIE* **1996**, *2853*, 149.
(5) *Nonlinear Optics*; Boyd, R. W., Ed.; Academic Press: New York, 1992.
(6) *Solid State Chemistry, An Introduction*; Smart, L., Moore, E., Eds.; Chapman and Hall: London, 1992.
(7) For leading references, see the following. Kobayashi, T. *Pure Appl. Chem.* **1995**, *67*, 387−400.
(8) Hein, J.; Bergner, H.; Lenzner, M.; Rentsch, S. *Chem. Phys.* **1994**, *179*, 543. (b) Thienpont, H.; Rikken, G. L. J. A.; Meijer, E. W.; ten Hoeve, W.; Wynberg, H. *Phys. Rev. Lett.* **1990**, *65*, 2141.
(9) Marder, S. R.; Torruellas, W. E.; Blanchard-Desce, M.; Ricci, V.; Stegeman, G. I.; Gilmour, S.; Brédas, J.-L.; Li, J.; Bublitz, G. U.; Boxer, S. G. *Science* **1997**, *276*, 1233.
(10) Whittall, I. R.; Humphrey, M. G.; Samoc, M.; Swiatkienicz, J.; Luther-Davies, B. *Organometallics* **1995**, *14*, 5493.
(11) Draganjac, M. E.; Rauchfuss, T. B. *Angew. Chem., Int. Ed. Engl.* **1985**, *24*, 742.
(12) Sheik-Bahae, M.; Said, A. A.; Wei, T.-H.; Hagan, D. J.; Van Stryland, E. W. *IEEE J. Quantum Electron.* **1990**, *26*, 760. Values given here are in SI units. To convert to esu, the following conversion is used:

$$\chi^{(3)}_{\mathrm{esu}} = \frac{(3 \times 10^4)^2}{4\pi\epsilon_0}\chi^{(3)}_{\mathrm{SI}}$$

(13) Winter, C. S.; Oliver, S. N.; Manning, R. J.; Rush, J. D.; Hill, C. A. S.; Underhill, A. E. *J. Mater. Chem.* **1992**, *2*, 443.
(14) *W* and *T* are used in the literature. We wanted to define figures of merit whose terminology was consistent with this prior use, yet express them in such a way as to be intensity-independent and large when favorable.
(15) Galloway, C. P.; Doxsee, D. D.; Fenske, D.; Rauchfuss, T. B.; Wilson, S. R.; Yang, X. *Inorg. Chem.* **1994**, *33*, 4537.
(16) Yu, L.; Zhu, D. *Phosphorus, Sulfur Silicon Relat. Elem.* **1996**, *116*, 225.
(17) Dance, I. G.; Choy, A.; Scudder, M. L. *J. Am. Chem. Soc.* **1984**, *106*, 6285.
(18) Compton, D. L.; Brandt, P. F.; Rauchfuss, T. B.; Rosenbaum, D. F.; Zukoski, C. F. *Chem. Mater.* **1995**, *7*, 2342.
(19) Steimecke, G.; Sieler, H. J.; Kirmse, R.; Hoyer, E. *Phosphorus Sulfur* **1979**, *7*, 49.
(20) Steimecke, G.; Sieler, H.-J.; Kirmse, R.; Dietzsch, W.; Hoyer, E. *Phosphorus Sulfur Relat. Elem.* **1982**, *12*, 237.
(21) Yang, X.; Rauchfuss, T. B.; Wilson, S. R. *J. Chem. Soc., Chem. Commun.* **1990**, 34.
(22) Dance, I. G. *Aust. J. Chem.* **1978**, *31*, 2195.
(23) Tian, J.-G.; Zang, W. P.; Zhang, C. Z.; Zhang, G. *Appl. Opt.* **1995**, *21*, 4331.
(24) Hughes, S.; Burzler, J. M.; Spruce, G.; Wherrett, B. S. *J. Opt. Soc. Am. B* **1995**, *12*, 1888.
(25) *Handbook of Nonlinear Optics*; Sutherland, R. L., Ed.; Marcel Dekker: New York, 1996.
(26) Zhao, M.-T.; Singh, B. P.; Prasad, P. N. *J. Chem. Phys.* **1988**, *89*, 5535.
(27) Tebbe, F. N.; Wasserman, E.; Peet, W. G.; Vatvars, A.; Mayman, A. C. *J. Am. Chem. Soc.* **1982**, *104*, 4971. Steuel, R. *Top. Curr. Chem.* **1982**, *102*, 149.
(28) Cassoux, P.; Valade, L.; Kobayashi, H.; Kobayashi, A.; Clark, R. A.; Underhill, A. E. *Coord. Chem. Rev.* **1991**, *110*, 115.
(29) Zuo, J.-L.; Yao, T.-M.; You, X.-Z.; Fun, H.-K.; Yip, B.-C. *J. Mater. Chem.* **1996**, *6*, 1633. Papadopoulos, M. G.; Waite, J.; Winter, C. S.; Oliver, S. N. *Inorg. Chem.* **1993**, *32*, 277 and references therein.
(30) Scheithauer, S.; Mayer, R. *Thio- and Dithiocarboxylic Acids and Their Derivatives in Topics in Sulfur Chemistry*; Senning, A., Ed.; Thieme: Stuttgart, 1979; pp 2−4.
(31) Long, N. J. *Angew. Chem., Int. Ed. Engl.* **1995**, *34*, 826.
(32) Compton, D. L.; Brandt, P. F.; Rauchfuss, T. B.; Rosenbaum, D. F.; Zukoski, C. F. *Chem. Mater.* **1995**, *7*, 2342.
(33) Manners, I. *Angew. Chem., Int. Ed. Engl.* **1996**, *35*, 1602.
(34) Hou, H.-W.; Xin, X.-Q.; Shi, S. *Coord. Chem. Rev.* **1996**, *153*, 25.
(35) Shi, S.; Zhang, X.; Shi, X. F. *J. Phys. Chem.* **1995**, *99*, 14911.
(36) Verma, A. K.; Rauchfuss, T. B.; Wilson, S. R. *Inorg. Chem.* **1995**, *34*, 3072.
(37) For an overview of the area, see the following. Dance, I.; Fisher, K. *Prog. Inorg. Chem.* **1994**, *41*, 637.